

^{31}P Solid-State Nuclear Magnetic Resonance Spectroscopy of Aluminum Phosphate Minerals

William F. Bleam^{1,2}, Philip E. Pfeffer¹ and James S. Frye³

¹ Eastern Regional Research Center, USDA-ARS, 600 E. Mermaid Lane, Philadelphia, PA 19118, USA

² Current Address: Department of Soil Science, 1525 Observatory Drive, University of Wisconsin-Madison, Madison, WI 53706, USA

³ Department of Chemistry, Colorado State University Regional NMR Center, Colorado State University, Fort Collins, CO 80523, USA

Abstract. This study examines the links between ^{31}P solid-state NMR studies of aluminum phosphate minerals and their crystallographic structures. We found that ^{31}P isotropic chemical shift values, δ_{iso} , carry little information about mineral structures. There seems to be no relation between the chemical shift anisotropy, $\Delta\delta = \delta_{33} - \delta_{11}$ ($\delta_{33} > \delta_{22} > \delta_{11}$), and indices of phosphate-tetrahedra distortion. ^{31}P - ^1H heteronuclear magnetic dipole interactions, on the other hand, carry important information about hydrous phosphate mineral structures, information that should prove to be quite valuable in studies of phosphate adsorbed on mineral surfaces. This interaction can be measured through a variety of qualitative and quantitative experiments. It appears that spin diffusion is so rapid that subtle differences in hydrogen-bonding environments cannot be resolved.

Introduction

There are many circumstances when diffraction of short-wave-length particles (viz., x-rays, electrons or neutrons) cannot be used to determine a material's structure. For instance, the material lacks sufficient long-range order to give a diffraction pattern suitable for least-squares structure refinement or because the material one is interested in occurs at an interface. High-resolution solid-state *nuclear magnetic resonance* (NMR) spectroscopy has proven extremely valuable for learning about structure under these circumstances (Andrew 1981, Fyfe et al. 1982, Fyfe et al. 1983, Kirkpatrick et al. 1985, Oldfield and Kirkpatrick 1985, Nagy et al. 1985).

We are primarily interested in using ^{31}P NMR to study the structure of orthophosphate adsorbed at the surface of aluminum oxide and aluminosilicate minerals. Toward this end, we need to develop the means for interpreting the ^{31}P NMR spectra of phosphate in such environments. A detailed ^{31}P NMR study of aluminophosphate minerals whose crystal structures are known provides an opportunity for developing principles relating structure and spectra. We hope these principles will aid the interpretation of ^{31}P NMR solid-state spectra from phosphate in unknown structural environments.

Literature Review

We will not review all of the ^{31}P NMR research relevant to phosphate minerals, however there are several studies

which represent critical advances in the spectroscopy of this class of minerals. The first high-resolution ^{31}P NMR spectra of phosphates were those for calcium phosphates, bone and dental minerals reported by Rothwell et al. (1980) and Herzfeld, et al. (1980). Using cross-polarization (Pines et al. 1973), magic-angle-spinning (CP-MAS) (Schaefer and Stejskal 1976) spectra (Figure 1b), Rothwell et al. (1980) varied the contact time to as a way of distinguishing resonances.

Tropp and coworkers (1983) illustrated the value of comparing Bloch-decay, magic-angle-spinning and CP-MAS spectra (Figures 1a and 1b) to highlight the effect of ^{31}P - ^1H interactions on spectra. This approach was extended considerably by Aue, Roufosse and coworkers (Aue et al. 1984, Roufosse et al. 1984) who added "interrupted decoupling" CP-MAS experiments (Opella and Frey 1979, Figure 1c) to the techniques used by Tropp, et al. (1983). The emphasis in these studies was the effect of protonation on phosphate- ^{31}P chemical shift anisotropy (CSA) and the possibility of using ^{31}P - ^1H dipole interactions to "edit" MAS NMR spectra.

Griffiths, et al. (1986), in their ^{31}P study of ortho- and polyphosphates, found the trend toward a downfield shift of δ_{iso} with increasing protonation does not hold in all cases. It is important to remember that these and other exceptions reduce the confidence we can place in conclusions drawn from a parameter such as δ_{iso} . Cheetham, et al. (1986) suggested the weak correlation between δ_{iso} and the mean P-O bond length arises because the "paramagnetic" term in the shift tensor dominates the "diamagnetic" term. A close linear correlation between δ_{iso} and the mean $\angle \text{Al}-\text{O}-\text{P}$ bridging bond angle in the "quartz" polymorphs of AlPO_4 ($r = 0.9984$) was found by Müller, et al. (1984), but the utility of this parameter has not been investigated for aluminum phosphates where the Al(III) is in octahedral rather than tetrahedral coordination.

The principal components of the chemical shift tensor (δ_{ii} , $i = 1, 2, 3$) distinguish three classes of symmetry: "isotropic" (point-groups T_d ($\bar{4}3m$) or O_h ($m\bar{3}m$)), "axial" (point-groups containing C_n (n), $n \geq 3$, as a subgroup), or "anisotropic" (all other point groups). Grimmer (1978) found that the shielding anisotropy was correlated with the mean P-O bond length for various phosphorus-containing compounds and select phosphates. Minerals containing protonated phosphate anions, such as monetite [CaHPO_4] and brushite [$\text{CaHPO}_4 \cdot 2\text{H}_2\text{O}$], display intense spinning-side bands to several orders (Rothwell et al. 1980), a clear indication of a relatively large CSA (Maricq and Waugh

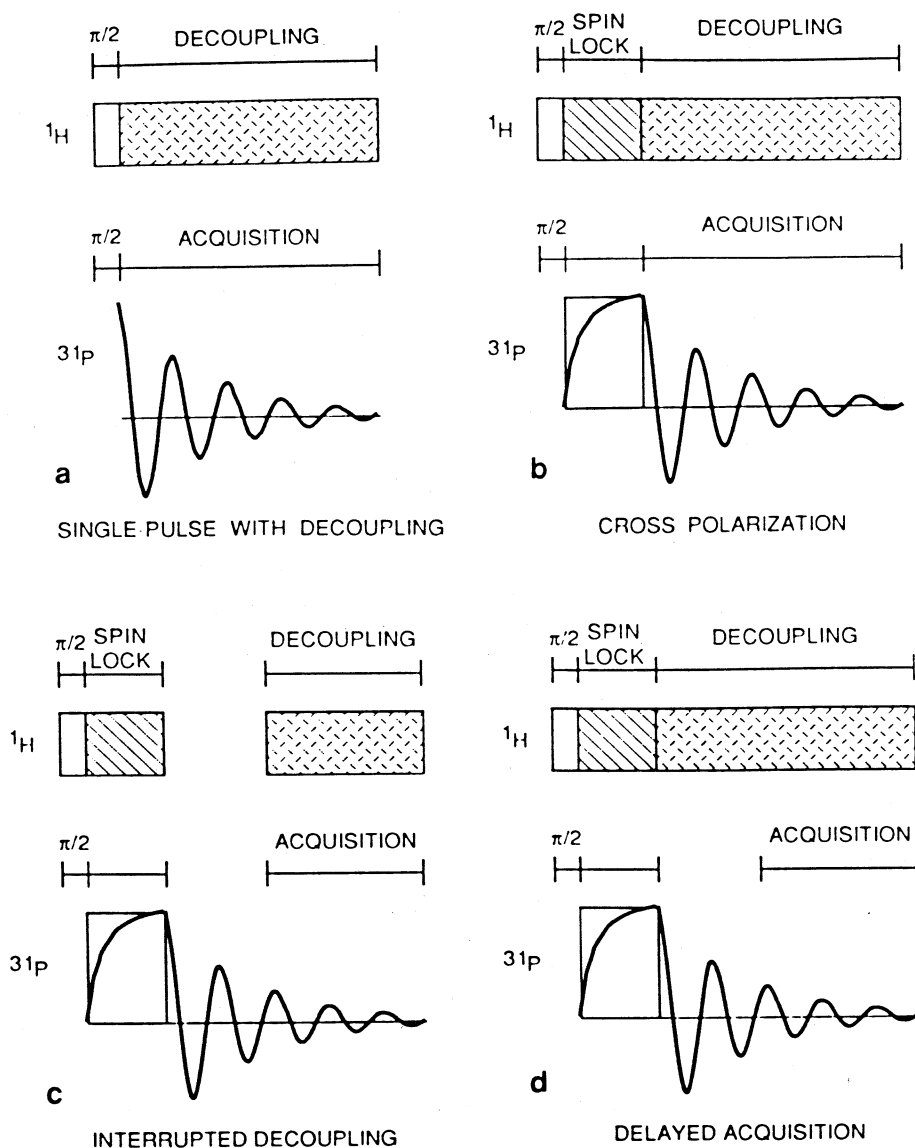


Fig. 1 a-d. Pulse sequences for various solid-state nuclear magnetic resonance experiments showing both ^1H and ^{31}P channels:
a) single-pulse, magic-angle-spinning with high-power, $^{31}\text{P}-^1\text{H}$ decoupling;
b) cross-polarization, magic-angle-spinning with high-power, $^{31}\text{P}-^1\text{H}$ decoupling;
c) cross-polarization, magic-angle-spinning with "interrupted" high-power, $^{31}\text{P}-^1\text{H}$ decoupling;
d) "delayed acquisition" cross-polarization, magic-angle-spinning with high-power, $^{31}\text{P}-^1\text{H}$ decoupling

1979, Herzfeld and Berger 1980). CSA has been shown repeatedly to be an important NMR parameter for phosphate minerals (Grimmer and Haubenreisser 1983, Tropp et al. 1983, Duncan and Douglass 1984, Mudrakovskii et al. 1985, Cheetham et al. 1986, Griffiths et al. 1986).

Although direct protonation of phosphate oxygens does not occur in any of the minerals included in our study, detailed examination of the mineral structures demonstrate H-bonding significantly affects P-O bond lengths. These structural effects are, however, subtle and one cannot make sweeping generalizations. After all, H-bonding is not the only factor influencing crystal structure. For clarity, we denote the length of those P-O bonds whose oxygens receive H-bonds as " $d(\text{P}-\text{O}[\dots\text{H}])$ " and those *not* receiving H-bonds simply as " $d(\text{P}-\text{O})$ ".

The length of those P-O bonds whose oxygens receive H-bonds, $d(\text{P}-\text{O}[\dots\text{H}])$, in variscite (Kniep et al. 1977), senegalite (Keegan et al. 1979), and brazilianite (Gatehouse and Miskin 1974) fall in the range 1.538 Å to 1.546 Å, while $d(\text{P}-\text{O})$ in these same minerals fall in the range 1.514 Å to 1.528 Å. In every case, the differences between $d(\text{P}-\text{O}[\dots\text{H}])$ and $d(\text{P}-\text{O})$ are highly significant (Cruickshank and Robertson 1953).

Crandallite (Blount 1974) and lazulite (Giuseppetti and Tadini 1983) stand in apparent opposition to this analysis, $d(\text{P}-\text{O}[\dots\text{H}])$ ranges from 1.512 Å to 1.520 Å while $d(\text{P}-\text{O})$ is in the range 1.542 Å to 1.543 Å. This reversal, viz., $d(\text{P}-\text{O}[\dots\text{H}]) < d(\text{P}-\text{O})$, in crandallite and lazulite can be easily rationalized. The H-bonded phosphate oxygen in crandallite does not coordinate Al(III) leaving greater electron density on that oxygen for a stronger (and shorter) P-O bond, i.e., that oxygen is underbonded. The two long P-O bonds in lazulite involve oxygens coordinating both Al(III) and Mg(II) while the short P-O bonds coordinate only one Al(III) and receive a weak bifurcated H-bond. The short P-O bonds in lazulite arise because the oxygens coordinating only one Al(III) are relatively underbonded (Giuseppetti and Tadini 1983).

P-O bond lengths in wavellite fall in the range 1.518 Å to 1.530 Å (Araki and Zoltai 1968), which can be compared to $1.514 \text{ Å} < d(\text{P}-\text{O}) < 1.528 \text{ Å}$ in variscite, senegalite and brazilianite. Recall $d(\text{P}-\text{O}[\dots\text{H}])$ falls in the range 1.538 Å to 1.546 Å in the latter minerals. We applied Cruickshank and Robertson's (1953) statistical method to P-O bonds in wavellite and found that the probability that any two P-O bond lengths were equal always exceeded 0.05, i.e.,

the P–O bond lengths in wavellite are statistically indistinguishable. Furthermore, the possibility that phosphate oxygens in wavellite could be underbonded in the manner described for crandallite and lazulite does not arise. We conclude, therefore, that either no H-bonding occurs in wavellite or it is limited to weak bifurcated H-bonds.

Variscite and wavellite are two aluminum phosphate minerals which are thought to form in soils, surface waters and sediments (Leckie and Stumm 1970, Nriagu 1976, Goldschmidt and Rubin 1978, Vielillard et al. 1979). Given our preceding discussion of H-bonding in these minerals, an important test of the capability of ^{31}P solid-state NMR to discriminate a structurally important characteristic of aluminum phosphates presents itself in the ^{31}P – ^1H dipolar interaction in variscite and wavellite.

There are a variety of experiments which yield information about ^{31}P – ^1H interactions. Among these are qualitative CP-MAS “interrupted decoupling” experiments (Opella and Frey 1979, Aue et al. 1984, Roufousse et al. 1984) and quantitative CP-MAS (Pines et al. 1973, Schaefer and Stejskal 1976) experiments where the cross-polarization relaxation time, T_{PH} , is measured (Maciel and Sindorf 1980, Fyfe et al. 1982, Grimmer et al. 1986). The former is a modified CP-MAS experiment in which a short time interval is inserted between the end of the spin-lock phase and re-application of high-power proton decoupling (Figures 1b and 1c). As with the conventional CP-MAS experiment,

acquisition of the free-induction decay (FID) curve occurs during high-power decoupling.

Experimental Methods and Materials

Experimental Methods

The solid-state NMR spectra were collected at the Colorado State University Regional NMR Center. All spectra were collected at 60.745 MHz on a modified Nicolet N-150 NMR spectrometer.

The total number of paramagnetic spins in the aluminum phosphates were measured by integrating the peak area from *electron paramagnetic resonance* (EPR) spectra and comparing these with peak-area measurements of a National Bureau of Standards ruby ([Cr(III):Al₂O₃, Standard Reference Material # 2601). EPR measurements were made with a Varian Model E-109B spectrometer.

Aluminum Phosphate Minerals

The minerals used in this study are listed in Table 1. The aluminophosphate zeolite, AlPO₄-5, is a product of Union Carbide Corporation. The remaining minerals are from the Department of Mineral Sciences, National Museum of Natural History, Smithsonian Institution, Washington, DC. All minerals were ground to a powder.

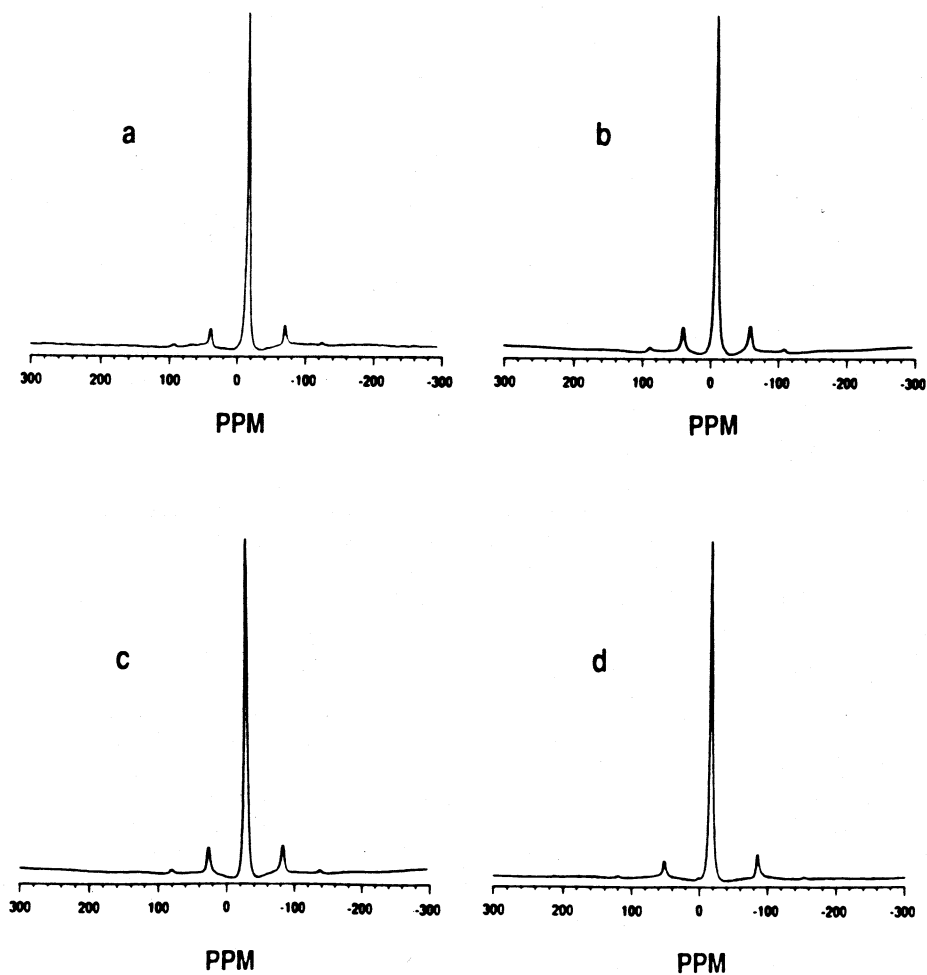


Fig. 2a–d. 60.754 MHz ^{31}P solid-state NMR spectra (CP-MAS with high-power, ^{31}P – ^1H decoupling) with 85 percent H_3PO_4 used as an external reference:

- a) variscite [NMNH # 87484-5] (64 scans, 2 k data points, 20 kHz spectral width, 1 s recycle time, 0.5 ms contact time);
- b) wavellite [NMNH # R16042] (1000 scans, 4 k data points, 20 kHz spectral width, 1 s recycle time, 0.5 ms contact time);
- c) augelite [NMNH # 137305] (376 scans, 2 k data points, 20 kHz spectral width, 1 s recycle time, 0.5 ms contact time);
- d) senegalite [NMNH # 137180] (52624 scans, 4 k data points, 20 kHz spectral width, 1 s recycle time, 1 ms contact time)

Table 1. Aluminum phosphate minerals used in this study

Mineral	Identification	Formula	Space group
Variscite	NMNH # 87484-5	$\text{AlPO}_4 \cdot 2\text{H}_2\text{O}$	<i>Pbca</i>
Wavellite	NMNH # R16042	$\text{Al}_3(\text{OH})_3(\text{PO}_4)_2 \cdot 5\text{H}_2\text{O}$	<i>Pcmm</i>
Senegalite	NMNH # 137180	$\text{Al}_2(\text{OH})_3(\text{PO}_4) \cdot \text{H}_2\text{O}$	<i>P2_1nb</i>
Augelite	NMNH # 137305	$\text{Al}_2(\text{OH})_3\text{PO}_4$	<i>C2/m</i>
Berlinite	NMNH # 144881	AlPO_4	<i>P3_121</i>
Zeolite	Union carbide	$\text{TPAOH} \cdot 12\text{AlPO}_4 \cdot 5\text{AlPO}_4 \cdot 5$	<i>P6cc</i>
Brazilianite	NMNH # 148251	$\text{NaAl}_2(\text{OH})_4(\text{PO}_4)_2$	<i>P2_1/n</i>
Crandallite	NMNH # 104085-2	$\text{CaAl}_3(\text{OH})_6(\text{PO}_4)_3$	<i>R\bar{3}m</i>
Lazulite	NMNH # 45770-1	$\text{MgAl}_2(\text{OH})_2(\text{PO}_4)_2$	<i>P2_1/c</i>

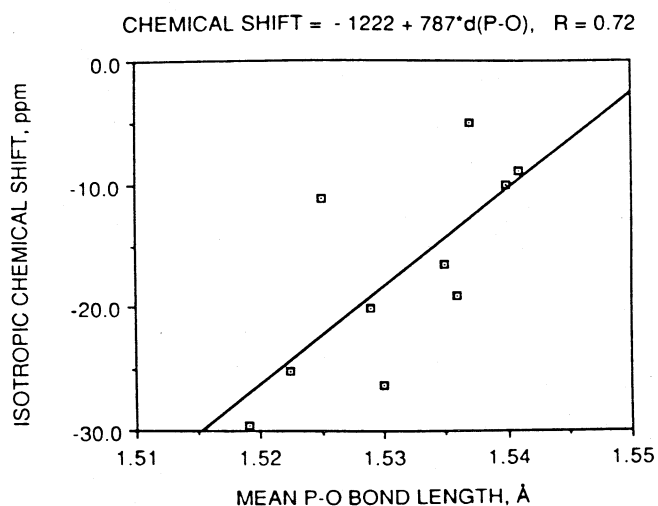
Experimental Results

1. Chemical Shift and Crystal Structure

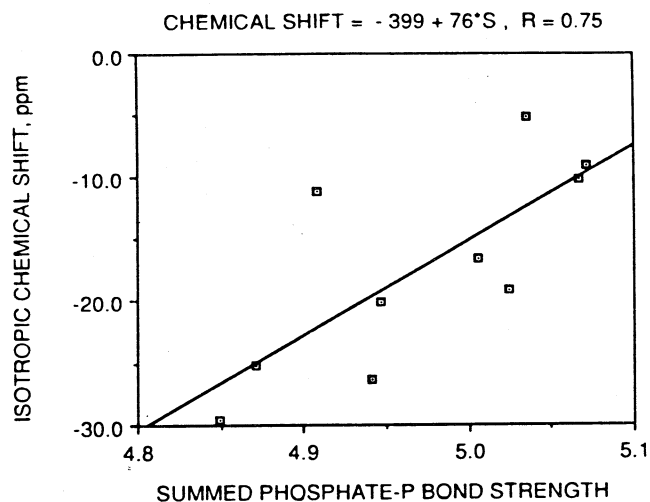
The ^{31}P CP-MAS spectra of the minerals variscite, wavellite, augelite and senegalite appear in Figure 2. These four aluminum phosphates represent an interesting range of structures. All of the Al(II) in variscite and wavellite exists in 6-fold coordination (Araki and Zoltai 1968, Kniep et al. 1977). Half of the Al(III) in augelite and senegalite is in 5-fold coordination and half in 6-fold (Araki et al. 1968, Keegan et al. 1979). The Al(III) coordination polyhedra form chains cross linked by phosphate in wavellite and senegalite. The Al(III) coordination polyhedra in variscite and augelite, however, do not form subunits of infinite extent. Single Al(III) coordination octahedra in variscite and edge-sharing tetramers of Al(III) polyhedra in augelite are cross-linked by corner-sharing phosphate tetrahedra. Interestingly, the ^{31}P CP-MAS spectra for these minerals all look pretty much the same.

There is a weak correlation between the mean P–O bond length, $\langle d(\text{P}-\text{O}) \rangle$, (Figure 3a) or the Brown and Shannon (1973) total P–O bond strength (Figure 3b) and the isotropic chemical shift. Only about 50 percent of the variation in δ_{iso} can be explained by changes in $\langle d(\text{P}-\text{O}) \rangle$. Given the near constancy in $\langle d(\text{P}-\text{O}) \rangle$ and mean $\angle \text{O}-\text{P}-\text{O}$ (Cruickshank 1961, Louisnathan and Gibbs 1972), $\langle \angle \text{O}-\text{P}-\text{O} \rangle$, this is not surprising. The correlation between isotropic chemical shift and the mean atomic valence of the phosphate oxygen (Baur 1970) was weaker than those mentioned above ($r=0.31$). We did not include a figure illustrating the relationship since the correlation was so low.

Using the method of Herzfeld et al. (1980), we made estimates of the principal components of the chemical shift tensor and present these in Table 2. The uncertainties in the principal components of the shift tensors appearing in Table 2 arise from graphical technique of Herzfeld et al. (1980) and have no statistical significance. These uncertainties bear no relation to the experimental error in the measurement of the isotropic chemical shift from MAS spectra. The estimates were made using spinning-side-band intensities measured at a single spinning frequency. Spinning rates were in the range of 3 to 4 kHz. Selected CP-MAS spectra from which the shift tensor elements were determined appear in Figure 4. Notice that lazulite, which has the greatest chemical shift anisotropy ($\Delta\delta = \delta_{33} - \delta_{11}$, $\delta_{33} \geq \delta_{22} \geq \delta_{11}$), has intense spinning-sidebands up to third order. The an-



a



b

Fig. 3a, b. ^{31}P isotropic chemical shift (ppm) versus (a) the mean P–O bond length and (b) the summed Brown and Shannon (1973) P–O bond strength for the aluminum phosphate minerals used in this study

isotropy can clearly be seen in the berlinite spectra even though only first-order spinning-sidebands are discernible.

Since the CSA reflects symmetry, one may imagine that a relation exists between some measure of distortion and CSA. The coefficient of variation (i.e., the mean divided by the standard deviation) in the P–O bond lengths or the $\angle \text{O}-\text{P}-\text{O}$ bond angles gives a crude indication of distortion. As can be seen in Figure 5, there is no relationship between P–O bond-length distortions of the phosphate and CSA, at least for the minerals we studied. The relation between the coefficient of variation in $\angle \text{O}-\text{P}-\text{O}$ bond angles and CSA is similar to the bond length case. Root mean-square relative deviation, used by others to estimate distortion (Brown and Shannon 1973), gave the same picture as coefficient of variation.

A comparison between augelite and lazulite dramatically illustrates this point. The coefficients of variation in

Table 2. ^{31}P isotropic chemical shifts (δ_{iso}), principal components of the chemical shift tensors (δ_{ii} , $i=1, 2, 3$), and the anisotropy ($\Delta\delta = \delta_{33} - \delta_{11}$, $\delta_{33} > \delta_{22} > \delta_{11}$) for several aluminum phosphate minerals

Mineral	δ_{iso} (ppm)	δ_{11} (ppm)	δ_{22} (ppm)	δ_{33} (ppm)	$\Delta\delta$ (ppm)
Variscite	-19.2	-50 ± 10	-30 ± 20	22 ± 30	72 ± 6
Wavellite	-11.2	-54 ± 6	-15 ± 1	36 ± 8	90 ± 10
Senegalite	-16.2	-43 ± 3	-43 ± 3	36 ± 7	80 ± 10
Augelite	-29.6	-61 ± 9	-61 ± 9	30 ± 20	100 ± 30
Berlinite	-25.3	-60 ± 10	-60 ± 10	50 ± 20	110 ± 30
$\text{AlPO}_4\text{-5}$	-26.3	-53 ± 2	-53 ± 2	26 ± 7	79 ± 5
Brazilianite	-10.2	-47 ± 3	-24 ± 1	11 ± 9	57 ± 6
Crandallite	-5.2	40 ± 30	20 ± 20	-70 ± 10	100 ± 10
Lazulite	-20.1	-170 ± 50	30 ± 30	120 ± 60	290 ± 10

P—O bond lengths for augelite and lazulite are 1.0 percent and 1.1 percent respectively (Araki et al. 1968, Giuseppetti and Tadini 1983). The coefficients of variation in the $\angle\text{O—P—O}$ bond angles are 2.5 percent and 2.0 percent for augelite and lazulite, respectively. If the actual distortion of the phosphate (either its bond lengths or angles) determined the magnitude of the components in the chemical shift tensor, the CSA of augelite and lazulite would be essentially the same. In reality, augelite has $\Delta\delta \approx 100$ ppm while $\Delta\delta \approx 300$ ppm for lazulite. One cannot attribute this large CSA to Fe(III) or other transition metal ions present in the lazulite since the probability that the number of paramagnetic spins in augelite ($8 \pm 5 (10^{14})$ spins per gram) equals those in lazulite ($2 \pm 1 (10^{15})$ spins per gram) exceeds 5 percent.

Incidentally, wavellite contains more paramagnetic centers ($6.0 \pm 0.3 (10^{15})$ spins per gram) than lazulite, yet the spinning-side bands are much more intense in lazulite (Figure 4c) than wavellite (Figure 4b).

There are two characteristics which distinguish lazulite. First, the magnitude of the elements in the *anisotropic-temperature-factor* tensor for the phosphorus in lazulite are more than two-orders of magnitude less than those in all other aluminum phosphates we studied (Giuseppetti and Tadini 1983). The temperature factor is a function describing the relative probability of finding the nucleus of an atom displaced from its equilibrium position. Second, each phosphate in lazulite is linked to two 6-fold coordinated Al(III) through shared edges (Giuseppetti and Tadini 1983). Phosphate share corners, at most, with the Al(III) coordination polyhedra in all other aluminum phosphates we studied.

In summary, one cannot make simple associations between the distortion of the phosphate tetrahedra and CSA. The large CSA observed in the calcium phosphates brushite or monetite (Herzfeld et al. 1980, Rothwell et al. 1980, Tropp et al. 1983, Aue et al. 1984) results from the *direct* protonation of the phosphate oxygen. Direct protonation of phosphate oxygens does not occur in lazulite (Giuseppetti and Tadini 1983), and therefore cannot explain the 300 ppm CSA.

II. $^{31}\text{P} - ^1\text{H}$ Heteronuclear Magnetic Dipole Interactions

Comparing Bloch-decay, magic-angle-spinning and CP-MAS spectra provides a means of qualitatively distinguishing resonances with different degrees of $^{31}\text{P} - ^1\text{H}$ interac-

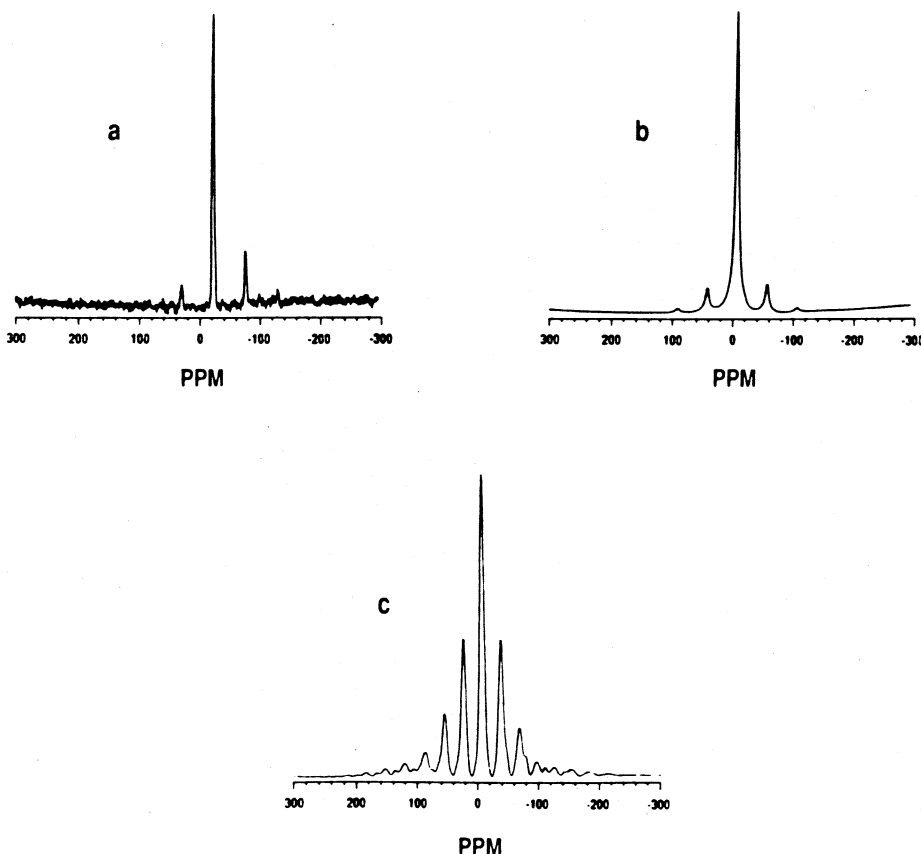


Fig. 4 a-c. 60.754 MHz ^{31}P solid-state NMR spectra (single-pulse, MAS with high-power, $^{31}\text{P} - ^1\text{H}$ decoupling) with 85 percent H_3PO_4 used as an external reference:

- a)** berlinite [NMNH # 144881] (40 scans, 4 k data points, 20 kHz spectral width, 60 s recycle time);
- b)** wavellite [NMNH # R16042] (1000 scans, 4 k data points, 20 kHz spectral width, 1 s recycle time);
- c)** lazulite [NMNH # 45770-1] (27000 scans, 2 k data points, 41.7 kHz spectral width, 1 s recycle time)

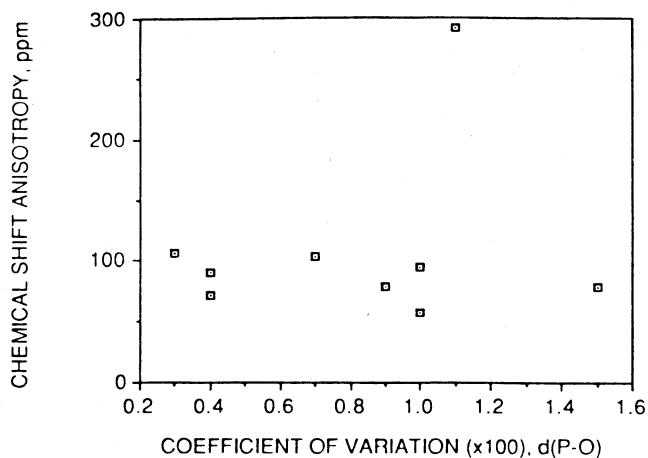


Fig. 5. Chemical shift anisotropy ($\Delta\delta = \delta_{33} - \delta_{11}$, $\delta_{33} > \delta_{22} > \delta_{11}$) in parts per million versus the coefficient of variation in the P-O bond lengths, expressed as percent, for the aluminum phosphate minerals used in this study

tion (Rothwell et al. 1980, Aue et al. 1984). Since there are no protons present in berlinite to couple with ^{31}P , the resonance appearing in the Bloch-decay, magic-angle-spinning spectrum of berlinite (Figure 6a) is absent in the CP-MAS spectrum (Figure 6b). A peak is apparent, however, in the CP-MAS spectrum of the Union Carbide aluminophosphate zeolite $\text{AlPO}_4\text{-5}$ (Figure 6d). That this peak is not

the same as the one appearing in the Bloch-decay, magic-angle-spinning spectrum can be seen from the different linewidth and δ_{iso} . The -22.3 ppm resonance prominent in the CP-MAS spectrum appears as a shoulder in the Bloch-decay, magic-angle-spinning spectrum (Figure 6c).

Another way of visualizing the strength of $^{31}\text{P}-^1\text{H}$ dipolar interaction is by comparing "decoupled" and "coupled" (i.e., with and without high-power, $^{31}\text{P}-^1\text{H}$ decoupling) Bloch-decay, magic-angle-spinning spectra (Figure 7). Lazulite and wavellite (Figures 7a and 7b) are examples of minerals characterized by relatively weak $^{31}\text{P}-^1\text{H}$ interactions. H-bonding in lazulite involving phosphate oxygens occurs through weak bifurcated H-bonds (Giuseppetti and Tadani 1983).

Spinning about the magic angle averages the dipolar interaction between spin = 1/2 nuclei (Andrew 1981). The spinning frequency must be much greater than the contribution to the line-width resulting from the dipolar interaction to significantly reduce broadening. The spinning frequencies used in our experiments ranged from 3 to 4.5 kHz, corresponding to $\approx 50\text{--}75$ ppm broadening at 60.745 MHz and were insufficient to completely average $^{31}\text{P}-^1\text{H}$ dipolar interaction. Note that $^{31}\text{P}-^1\text{H}$ dipolar interactions lead to broadening that is over *twice* as great as the range in isotropic chemical shifts (Figures 3a and 3b).

The results of a CP-MAS experiment on crandallite appear in Figure 8 and illustrate the magnitude of residual dipolar interaction under MAS. The "decoupled" data are from a variation of the conventional CP-MAS experiment

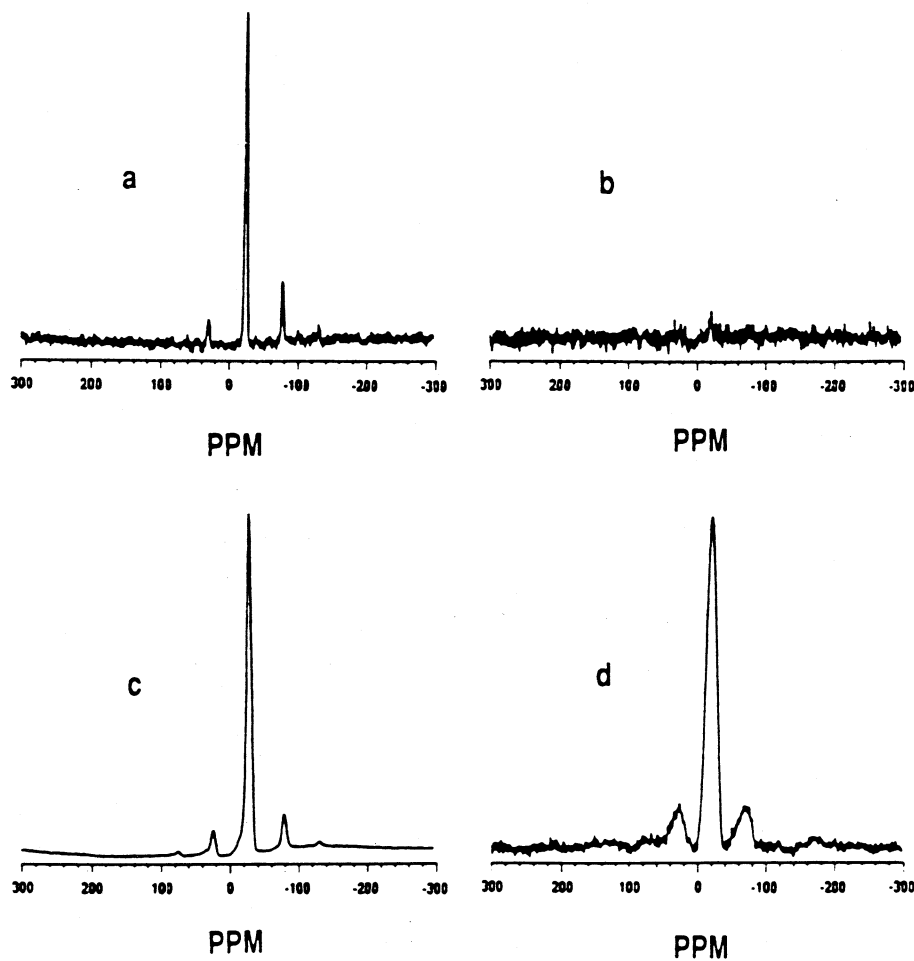


Fig. 6a-d. 60.754 MHz ^{31}P solid-state NMR spectra with 85 percent H_3PO_4 as an external reference:

- a)** berlinite [NMNH # 144881] (single-pulse, MAS with high-power, $^{31}\text{P}-^1\text{H}$ decoupling: 40 scans, 4 k data points, 20 kHz spectral width, 60 s recycle time;
- b)** berlinite [NMNH # 144881] (CP-MAS with high-power, $^{31}\text{P}-^1\text{H}$ decoupling: 5000 scans, 4 k data points, 20 kHz spectral width, 1 s recycle time, 0.5 ms contact time);
- c)** AlPO_4 zeolite [Union Carbide $\text{AlPO}_4\text{-5}$] (single-pulse, MAS with high-power, $^{31}\text{P}-^1\text{H}$ decoupling: 544 scans, 2 k data points, 20 kHz spectral width, 1 s recycle time);
- d)** AlPO_4 zeolite [Union Carbide $\text{AlPO}_4\text{-5}$] (CP-MAS with high-power, $^{31}\text{P}-^1\text{H}$ decoupling: 360 scans, 2 k data points, 20 kHz spectral width, 1 s recycle time, 0.5 ms contact time)

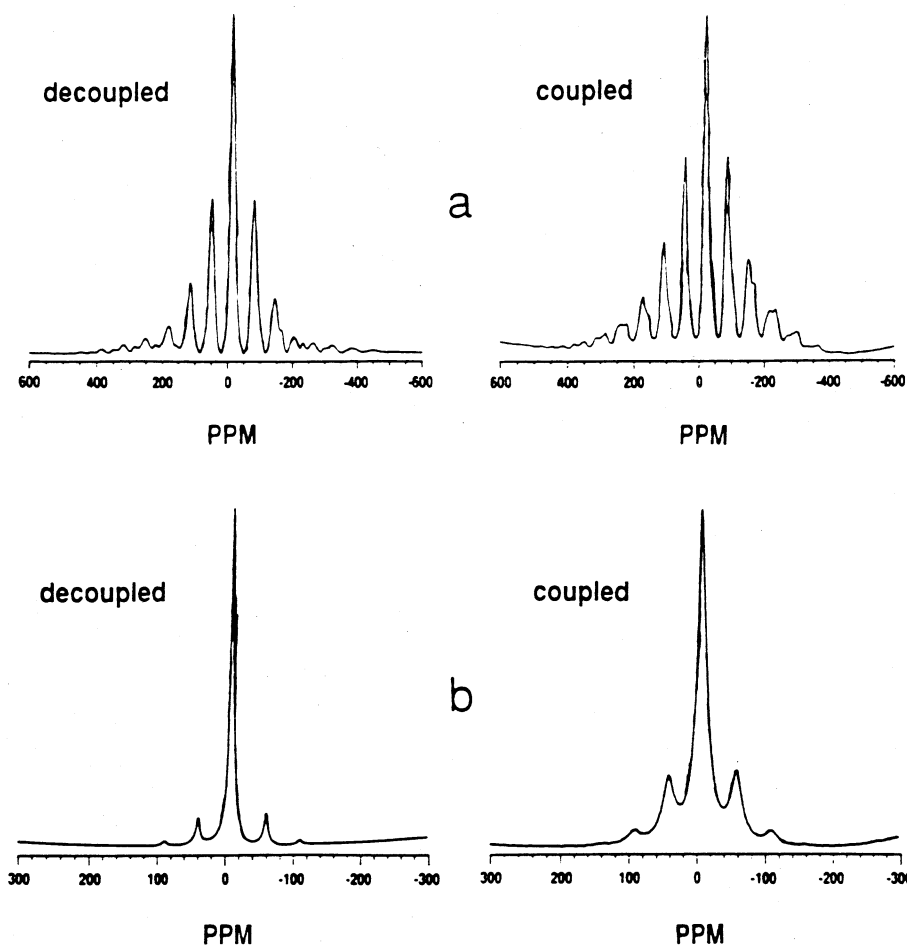


Fig. 7 a, b. 60.754 MHz ^{31}P solid-state NMR spectra (single-pulse, MAS with high-power, $^{31}\text{P}-^1\text{H}$ decoupling) with 85 percent H_3PO_4 used as an external reference:

a) lazulite [NMNH # 45770-1] ("decoupled": 27000 scans, 2 k data points, 41.7 kHz spectral width, 1 s recycle time; "coupled": 9000 scans, 2 k data points, 41.7 kHz spectral width, 1 s recycle time);

b) wavellite [NMNH # R16042] ("decoupled": 1000 scans, 4 k data points, 20 kHz spectral width, 1 s recycle time; "coupled": 1000 scans, 4 k data points, 20 kHz spectral width, 1 s recycle time)

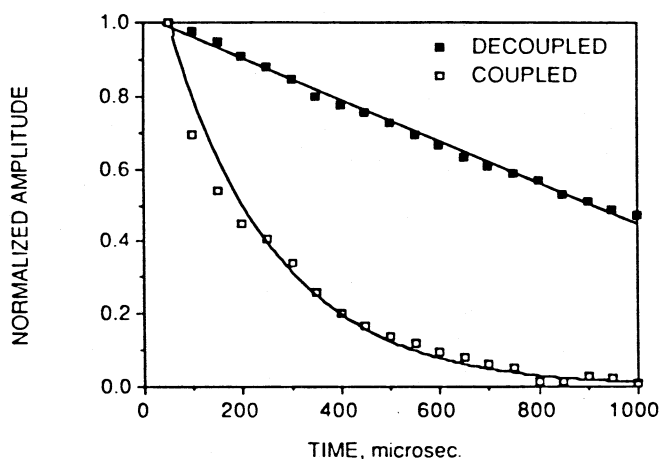


Fig. 8. ^{31}P cross-polarization, magic-angle spinning measurements on crandallite at 60.745 MHz: delayed acquisition under high-power ^1H decoupling ("decoupled") and "interrupted decoupling" ("coupled"). Amplitudes are normalized by the initial measurement

in which high-power, $^{31}\text{P}-^1\text{H}$ decoupling is continued following the cross-polarization contact-time but initiation of FID acquisition is delayed (Figure 1 d). The "coupled" data are acquired from yet another variation of the CP-MAS experiment. In the "coupled" experiment, a variable time interval inserted between the termination of spin locking and initiation of high-power, $^{31}\text{P}-^1\text{H}$ decoupling (Fi-

gure 1 c). Thus, acquisition in both experiments is under high-power $^{31}\text{P}-^1\text{H}$ decoupling the only difference is whether decoupling is continuous ("decoupled") or interrupted ("coupled") following spin lock.

It is clear from the data in Figure 8 that $^{31}\text{P}-^1\text{H}$ interaction can dramatically degrade the ^{31}P resonance in a hydrous aluminum phosphate mineral. Any attempt to quantify this interaction should be performed on a static sample since spinning the sample removes some of the interaction. Of course, if one is careful to perform the experiments under the same conditions, MAS results for different materials can be compared to one another.

A static cross-polarization experiment similar to the one described above for crandallite was performed on wavellite, the results appearing in Figure 9. We have plotted the *logarithm* of the amplitude rather than the normalized amplitude as we had done in Figure 8. Even on a logarithmic scale the "decoupled" (i.e., delayed acquisition with continuous decoupling) and the "coupled" (i.e., interrupted decoupling) amplitudes are quite different. It is clear that $^{31}\text{P}-^1\text{H}$ dipolar interaction is having a measureable effect on the spectrum of wavellite although there is little or no H-bonding.

Dipolar dephasing of ^{31}P nuclei by ^1H nuclei, the basis of the "interrupted decoupling" experiment, does not require that the phosphate oxygen receive a H-bond. The issue before us, however, is not whether $^{31}\text{P}-^1\text{H}$ dipolar interaction are present but if there is an NMR experiment capable of discriminating between phosphates on the basis

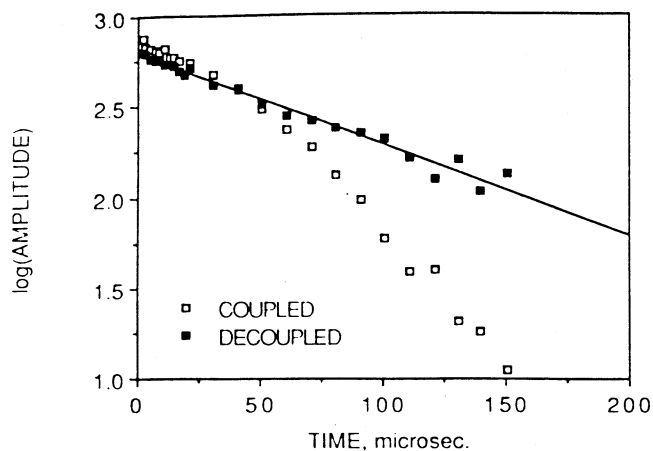
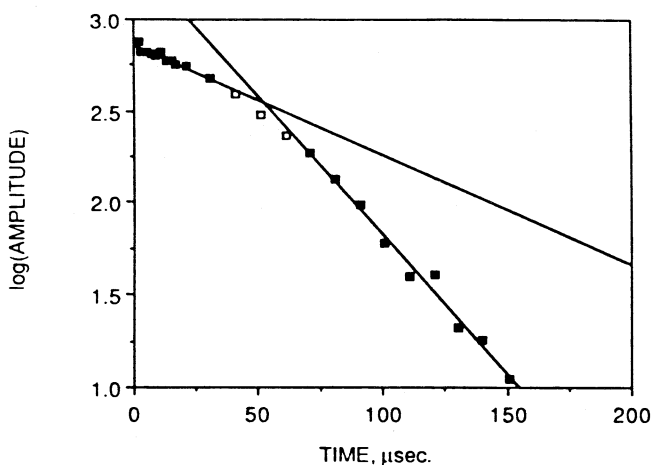
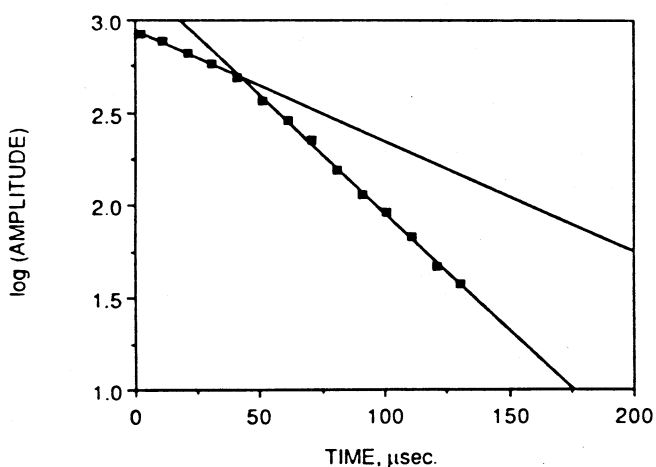


Fig. 9. Static, 60.745 MHz ^{31}P cross-polarization measurements on wavellite: delayed acquisition under high-power ^1H decoupling (decoupled) and "interrupted decoupling" (coupled)

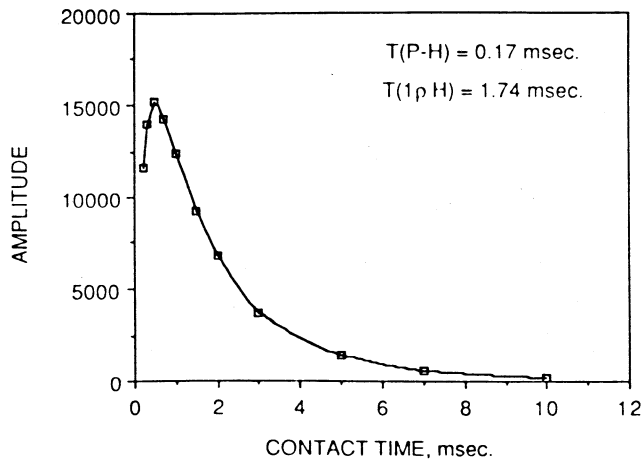


a

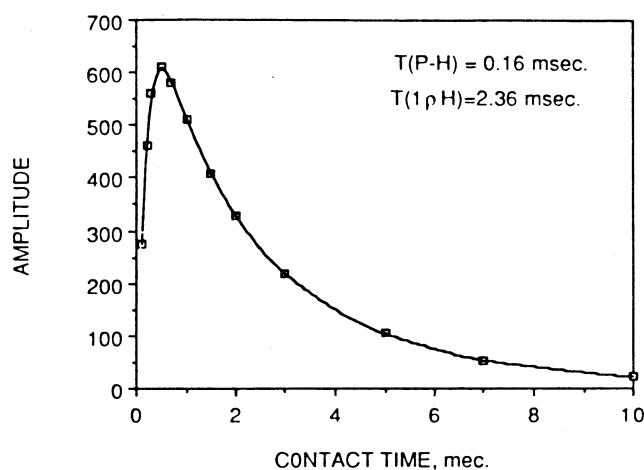


b

Fig. 10a, b. Static, 60.754 MHz ^{31}P cross-polarization experiment with "interrupted decoupling". Logarithm of the amplitude plotted versus the duration of the interrupt: (a) wavellite (the open squares were not included in the least-squares fitting of the data to linear models) and (b) variscite



a



b

Fig. 11a, b. Variable-contact-time, cross-polarization, magic-angle spinning ^{31}P experiment: (a) wavellite, spinning frequency ≈ 3 kHz and (b) crandallite, spinning frequency ≈ 3.5 kHz

of their H-bonding characteristics, a phenomena which clearly has a significant influence on P—O bond lengths.

Data from "interrupted decoupling" experiments on wavellite and variscite appear in Figures 10a and 10b. Some of the data for wavellite also appears in Figure 9, but in Figure 10a we have plotted linear regression models. It appears that the data for both wavellite and variscite can be fitted by two linear equations, one for interrupt intervals probing short-range interactions (interrupt $< 50 \mu\text{s}$) and one for those intervals probing relatively long-range interactions (interrupt $> 50 \mu\text{s}$).

Recalling that three of the phosphate oxygens in variscite receive H-bonds while none of the phosphate oxygens in wavellite are H-bond receivers, note that the slopes of the regression lines are similar. In fact, they are statistically indistinguishable. We must conclude that the "interrupted decoupling" experiment, where we were probing H-bonding characteristics using ^{31}P — ^1H dipolar interactions, does not discriminate between these minerals.

"Interrupted decoupling" CP-MAS experiments, of the type shown in Figures 8–10, should be considered qualita-

tive measurements of the $^{31}\text{P}-^1\text{H}$ dipolar interaction. Another measure of $^{31}\text{P}-^1\text{H}$ dipolar interaction is the cross-relaxation time, T_{PH} , determined from a variable contact-time experiment. The cross-relaxation time indicates the time scale of spin diffusion from the protons to the phosphorus nuclei. Results of two variable contact-time experiments on wavellite and crandallite appear in Figures 11a and 11b. Cross-relaxation times are best measured in "short"-contact-time experiments covering time intervals beginning at 50 μs and going as high as 10 ms.

The rate at which resonance amplitude increases (typically from 50 μs to 1 ms) is determined by the efficiency of cross-relaxation while the rate of amplitude decrease depends on the longitudinal relaxation rates of both the proton and the phosphorus nuclei, $T_{1\text{pH}}$ and $T_{1\text{pP}}$ respectively (Maciel and Sindorf 1980, Fyfe et al. 1982, Grimmer et al. 1986). Measurement of $T_{1\text{pH}}$ and $T_{1\text{pP}}$ in separate experiments reveal whether or not the decay of signal amplitude in a contact-time experiment is dominated by $T_{1\text{pH}}$. The efficiency of cross-relaxation in a CP-MAS experiment depends on how well the experimenter has fulfilled the Hartmann-Hahn condition during the spin-lock phase (Pines et al. 1973) and the rate of spinning. Large-amplitude, fast motion of the \mathbf{r}_{PH} vector makes T_{PH} (or T_{IS} in general) more sensitive to Hartmann-Hahn mismatch (Stejskal et al. 1977). Since magic-angle spinning averages dipolar interactions (Andrew 1981), cross-relaxation efficiency decreases as the spinning frequency increases. The cross-relaxation efficiency is expressed through the cross-relaxation time, i.e. T_{PH}^{-1} .

The cross-relaxation efficiency is the same for wavellite and crandallite (Figure 11a). Thus, although the phosphate oxygen not coordinating Al(III) in crandallite is involved in a complex H-bonding network involving four protons while none of the phosphate oxygens in wavellite receive H-bonds, the $^{31}\text{P}-^1\text{H}$ dipolar interactions, insofar as it influences cross-relaxation, seems to be the same. A material with strong dipolar interactions could lose cross-relaxation efficiency if the internuclear P-H vectors, $\mathbf{r}_{\text{P-H}}$, are motion-averaged on the time scale of the dipolar coupling.

Motion averaging of $\mathbf{r}_{\text{P-H}}$ is not the same physical phenomenon as the rotating-frame longitudinal relaxation of ^1H , $T_{1\text{pH}}$. The decay constant of a variable-contact-time curve is often equal to $T_{1\text{pH}}$, but contains a contribution from $T_{1\text{pP}}$. These two rotating-frame, longitudinal relaxation times can be measured independently in separate experiments. Because ^{31}P has a fairly large magnetogyric ratio, γ_{N} , and is 100 percent natural abundance, a complication with $T_{1\text{pH}} \approx T_{1\text{pP}}$ is more likely than, say, in the case of $^{13}\text{C}-^1\text{H}$ coupling.

We measured the number of paramagnetic spins in wavellite and crandallite using EPR. Wavellite [NMNH # R16042], with a $T_{1\text{pH}} \approx 1.7$ ms, contains $60 \pm 3(10^{14})$ spins per gram while crandallite [NMNH # 104085-2], with a $T_{1\text{pH}} \approx 2.4$ ms, contains $4 \pm 2(10^{14})$ spins per gram. The more rapid longitudinal relaxation rate of protons in wavellite may result from the higher content of paramagnetic spins.

Conclusions

We have seen that chemical information contained in the ^{31}P isotropic chemical shift is inconclusive. The difficulty in making unambiguous inferences about chemical struc-

ture from δ_{iso} could have been anticipated. Cruickshank (1961) commented on the near constancy of T-O bond lengths and $\angle\text{O-T-O}$ bond angles in second-row tetrahedral oxyanions. Clearly, if bond lengths and bond angles are virtually constant, it will be quite difficult to correlate δ_{iso} with either.

The magnitude of the individual principal elements of the chemical shift tensor suffer from the same limitations as their mean, δ_{iso} . As we saw earlier (Figure 5), it is also difficult to conceive of an index of distortion which correlates with the range in principal elements of the chemical shift tensor. Lazulite dramatically illustrates the potential pit-falls awaiting one who suggests that a large CSA indicates a large structural distortion of the phosphate tetrahedra.

In view of the strength of $^{31}\text{P}-^1\text{H}$ dipolar interactions, we are fortunate that protons exert such an important influence on the structures of inorganic phosphates. These interactions can be probed by a variety of ^{31}P NMR experiments (Opella and Frey 1979, Maciel and Sindorf 1980, Fyfe et al. 1982, Tropp et al. 1983, Aue et al. 1984, Roufosse et al. 1984, Grimmer et al. 1986). These experiments, especially the quantitative measurement of the cross-relaxation time, T_{PH} , represent the means for probing phosphate structure upon which we can rely with greatest confidence. Yet even this, our most promising experiment, cannot be regarded free of serious limitations.

Consider our experiments probing $^{31}\text{P}-^1\text{H}$ dipolar interactions in variscite, wavellite and crandallite where proton interactions with the phosphate oxygens operate at the level of H-bonding. "Interrupted decoupling" experiments could not distinguish wavellite from variscite based on dipolar interactions even though evidence based on crystal structures suggests that H-bonding differs in these two minerals.

In the final analysis, we have an enormously valuable resource in the minerals whose crystal structures are known. They provide an opportunity to test hypotheses and spectroscopic techniques, bringing the strengths and weaknesses of ^{31}P NMR spectroscopy of phosphate minerals and adsorbed phosphate into sharper focus.

Acknowledgements. The authors are grateful to the Colorado State University Regional NMR Center, funded by National Science Foundation Grant No. CHE-8616437. W.F.B. appreciates the generosity of Peter Dunn (Museum Specialist, Department of Mineral Sciences, Natural Museum of Natural History-Smithsonian Institution, Washington, DC) and J.M. Bennett (Union Carbide Corporation, Tarrytown, NY) who provided mineral samples used in this study.

References

- Andrew ER (1981) Magic angle spinning. *Int Rev Phys Chem* 1:195-224
- Araki T, Zoltai T (1968) The crystal structure of wavellite. *Z Kristallogr* 127:21-33
- Araki T, Finney JJ, Zoltai T (1968) The crystal structure of auge-lite. *Am Mineral* 53:1096-1103
- Aue WP, Roufosse AH, Glimcher MJ, Griffin RG (1984) Solid-state phosphorus-31 nuclear magnetic resonance studies of synthetic solid phases of calcium phosphate: Potential models of bone mineral. *Biochemistry* 23:6110-6114
- Baur, WH (1970) Bond length variation and distorted coordination polyhedra in inorganic crystals. *Trans Am Crystallogr Assoc* 6:129-155

- Blount AM (1974) The crystal structure of crandallite. *Am Mineral* 59:41-47
- Brown ID, Shannon RD (1973) Empirical bond-strength - bond-length curves for oxides. *Acta Crystallogr* A29:266-282
- Cheetham AK, Clayden NJ, Dobson CM, Jakeman RJB (1986) Correlations between ^{31}P NMR chemical shifts and structural parameters in crystalline inorganic phosphates. *J Chem Soc Chem Commun* 195-197
- Cruickshank DWJ, Robertson AP (1953) The comparison of theoretical and experimental determinations of molecular structures, with application to naphthalene and anthracene. *Acta Crystallogr* 6:698-705
- Cruickshank DWJ (1961) The role of 3d-orbitals in π -bonds between (a) silicon, phosphorus, sulphur, or chlorine and (b) oxygen or nitrogen. *J Chem Soc London* 5486-5504
- Duncan TM, Douglass DC (1984) On the ^{31}P chemical shift anisotropy in condensed phosphates. *Chem Phys* 87:339-349
- Fyfe CA, Bemis L, Clark HC, Curtin D, Davies J, Drexler D, Dudley RL, Gobbi GC, Hartmen JS, Hayes P, Klinowski J, Lenkinski RE, Lock CJL, Paul IC, Rudin A, Tchir W, Thomas JM, Wasylischen FRS, Wasylischen RE (1982) Analytical chemical applications of high-resolution nuclear magnetic resonance spectroscopy of solids. *Phil Trans R Soc London Ser A* 305:591-607
- Fyfe CA, Bemis L, Clark HC, Davies JA, Gobbi GC, Hartmen JS, Hayes PJ, Wasylischen RE (1983) High-resolution magic angle spinning and cross-polarization magic angle spinning solid-state NMR spectroscopy. In: Chisholm MH (ed) *Inorganic Chemistry: Toward the 21st Century*. American Chemical Society, New York, pp 405-430
- Gatehouse BM, Miskin BK (1974) The crystal structure of brazilianite, $\text{NaAl}_3(\text{PO}_4)_2(\text{OH})_4$. *Acta Crystallogr* B30:1311-1317
- Giuseppetti G, Tadini C (1983) Lazulite, $(\text{Mg, Fe})\text{Al}_2(\text{OH})_2(\text{PO}_4)_2$: Structure refinement and hydrogen bonding. *Neues Jahrb Mineral Monatsh* 9:410-416
- Goldschmidt T, Rubin AJ (1978) Aqueous chemistry and precipitation of aluminum phosphate. In: Rubin AJ (ed) *Chemistry of Wastewater Technology*, Ann Arbor Sci Pub Inc, Ann Arbor, MI, pp 59-80
- Griffiths L, Root A, Harris RK, Packer KJ, Chippendale AM, Tromans FR (1986) Magic-angle spinning phosphorus-31 nuclear magnetic resonance of polycrystalline sodium phosphates. *J Chem Soc Dalton Trans* 2247-2251
- Grimmer A-R (1978) ^{31}P NMR and π bond in solid phosphorus compounds. *Spectrochim Acta* 34A:941
- Grimmer A-R, Haubenreisser U (1983) High-field static and MAS ^{31}P NMR: Chemical shift tensors of polycrystalline potassium phosphates $\text{P}_2\text{O}_5 \cdot x\text{K}_2\text{O}$ ($0 \leq x \leq 3$). *Chem Phys Lett* 99:487-490
- Grimmer A-H, Starke P, Mägi M (1986) Charakterisierung von Kieselgelen durch die ^1H - ^{29}Si -Kreuzpolarisations-Relaxationszeit T_{SiH} und die ^1H -Spin-Gitter-Relaxationszeit $T_{1\rho\text{H}}$. *Z Chem* 26:114-115
- Herzfeld J, Berger AE (1980) Sideband intensities in NMR spectra of samples spinning at the magic angle. *J Chem Phys* 73:6021-6030
- Herzfeld J, Roufosse A, Haberkorn RA, Griffin RG, Glimcher MJ (1980) Magic angle sample spinning in inhomogeneously broadened biological systems. *Phil Trans R Soc London Ser B* 289:459-469
- Keegan TD, Araki T, Moore PB (1979) Senegalite, $\text{Al}_2(\text{OH})_3(\text{H}_2\text{O})(\text{PO}_4)$, a novel structure type. *Am Mineral* 64:1243-1247
- Kirkpatrick RJ, Smith KA, Schramm S, Turner G, Yang W-H (1985) Solid-state nuclear magnetic resonance spectroscopy of minerals. *Ann Rev Earth Planet Sci* 13:29-47
- Kniep R, Mootz D, Vegas A (1977) Variscite. *Acta Crystallogr* B33:263-265
- Leckie J, Stumm W (1970) Phosphate precipitation. In: Gloyna EF, Eckenfelder WW (eds) *Water Quality Improvements by Physical and Chemical Processes*. University of Texas Press, Austin, TX, pp 236-249
- Louisnathan SJ, Gibbs GV (1972) Bond length variation in TO_4^{n-} oxyanions of the third row elements: T = Al, Si, P, S and Cl. *Mat Res Bull* 7:1281-1292
- Maciel GE, Siodorf DW (1980) Silicon-29 nuclear magnetic resonance study of the surface of silica gel by cross polarization and magic-angle spinning. *J Am Chem Soc* 102:7606-7607
- Maricq MM, Waugh JS (1979) NMR in rotating solids. *J Chem Phys* 70:3300-3316
- Mudrakovskii IL, Mastikhin VM, Shmachkova VP, Kotsarenko NS (1985) High-resolution solid-state ^{29}Si and ^{31}P NMR of silicon-phosphorus compounds containing six-coordinated silicon. *Chem Phys Lett* 120:424-426
- Müller D, Jahn E, Ladwig G, Haubenreisser U (1984) High-resolution solid-state ^{27}Al and ^{31}P NMR: Correlations between chemical shift and mean Al-O-P angles in AlPO_4 polymorphs. *Chem Phys Lett* 109:332-336
- Nagy JB, Engelhardt G, Michel D (1985) High resolution NMR on adsorbate-adsorbent systems. *Adv Colloid Interface Sci* 23:67-128
- Nriagu JO (1976) Phosphate - clay mineral relations in soils and sediments. *Can J Earth Sci* 13:717-736
- Oldfield E, Kirkpatrick RJ (1985) High-resolution nuclear magnetic resonance of inorganic solids. *Science* 227:1537-1544
- Opella SJ, Frey MH (1979) Selection of nonprotonated carbon resonances in solid-state nuclear magnetic resonance. *J Am Chem Soc* 101:5854-5856
- Pines A, Gibby MG, Waugh JS (1973) Proton-enhanced NMR of dilute spins in solids. *J Chem Phys* 59:569-590
- Rothwell WP, Waugh JS, Yesinowski JP (1980) High-resolution variable-temperature ^{31}P NMR of solid calcium phosphates. *J Am Chem Soc* 102:2637-2643
- Roufosse AH, Aue WP, Roberts JE, Glimcher MJ, Griffin RG (1984) Investigations of the mineral phases of bone solid-state phosphorus-31 magic angle spinning nuclear magnetic resonance. *Biochemistry* 23:6115-6120
- Schaefer J, Stejskal EO (1976) Carbon-13 nuclear magnetic resonance of polymers spinning at the magic angle. *J Am Chem Soc* 98:1031-1032
- Stejskal EO, Schaefer J, Waugh JS (1977) Magic-angle spinning and polarization transfer in proton-enhanced NMR. *J Magn Reson* 28:105-112
- Tropp J, Blumenthal NC, Waugh JS (1983) Phosphorus NMR study of solid amorphous calcium phosphate. *J Am Chem Soc* 105:22-26
- Vielillard P, Tardy N, Nahon D (1979) Stability fields of clays and aluminum phosphates: parageneses in lateritic weathering of argillaceous phosphatic sediments. *Am Mineral* 64:626-634